Wave–Wave Interaction of Unstable Baroclinic Waves*

JOSEPH PEDLOSKY

Woods Hole Oceanographic Institution, Woods Hole, MA 02543

LORENZO M. POLVANI

MIT-WHOI Joint Program in Physical Oceanography, Center for Meteorology and Physical Oceanography, MIT, Cambridge, MA 02139

(Manuscript received 27 June 1986, in final form 29 September 1986)

ABSTRACT

Two slightly unstable baroclinic waves in the two-layer Phillips model are allowed to interact with each other as well as the mean flow. A theory for small dissipation rates is developed to examine the role of wave–wave interaction in the dynamics of vacillation and aperiodicity in unstable systems.

It is shown that the form of the dissipation mechanism as well as the overall dissipation timescale determines the nature of the dynamics. In particular, dissipation proportional to potential vorticity is shown to expunge amplitude vacillation due to wave–mean flow interaction.

Wave–wave interaction, however, can yield amplitude vacillation. As the dissipation is decreased, the solutions evolve from steady waves (although propagating) to periodic vacillation until finally at small dissipation rates, chaotic behavior is obtained.

This occurs in a range of relative growth rates of the two waves which depends on the strength of the wave–wave and wave–mean flow interactions.

1. Introduction

Unstable baroclinic currents can spawn unstable, wavelike disturbances which, in finite amplitude, may be either steady (aside from a simple translation of phase) or exhibit vacillatory behavior. The appearance of vacillatory behavior has been observed in carefully controlled laboratory experiments (e.g., Hart, 1972, 1973) but the mechanism causing the observed vacillation is still imperfectly understood. Yet the general phenomenon is so interesting that it presents itself as an obvious theoretical challenge.

Part of the fascination of the phenomenon of vacillation is its connection with aperiodic or chaotic behavior. Ever since the pioneering work of Lorenz (1963), it has been clear that the phenomenon of vacillation embraces two types of behavior, i.e., periodic, limit-cycle oscillations and aperiodic or chaotic vacillation. The connection between steady, periodic, and chaotic behavior as a function of the parameters of a baroclinic flow remains poorly understood and the "route to chaos" may depend sensitively on perplexingly delicate aspects of the physical system not, at first sight, of obvious importance. It is thus probably fair to say that as a preliminary to a complete understanding of the dynamics of vacillation we are first presented with the challenge of describing and delimiting various mechanisms which may give rise to such behavior and to test the robustness of the dynamics to alterations in the underlying physics.

One of the earliest theoretical models of baroclinic instability which exhibited the full range of steady, periodic and chaotic behavior was described by Pedlosky and Frenzen (1980). This was a two-layer model on an f-plane in which the basic flow had only vertical shear. Friction acted on both upper and lower layers by virtue of Ekman layers on the two rigid horizontal boundary surfaces. Interfacial friction was not included since the model was meant to at least crudely represent a continuous flow for which an interior zone of high viscous dissipation seemed inappropriate. The model so analyzed was shown to be qualitatively similar to the original Lorenz equations (see below) and, indeed, the behavior of the systems exhibited the transition to chaos found for some parameters in the Lorenz system. Namely, the amplitude of the baroclinic wave pulsated in a periodic way when dissipation was very small and then exhibited a period-doubling sequence leading to chaos as the dissipation slightly increased. Finally, for larger dissipation, steady solutions were obtained.

However, it has been shown (Pedlosky, 1981) that this behavior is very sensitive to relatively minor changes in the physics of the model. The inclusion of a small β-effect or slightly differing parameterizations

* Woods Hole Oceanographic Institution Contribution No. 6304.

of dissipation in the two layers is sufficient to expunge the so-called strange attractor and render all finite-amplitude solutions steady. The dynamics is thus *structurally unstable;* small, seemingly innocuous alterations in the physical model lead to O(1) changes in the long-time behavior of the wave field. Furthermore, the more recent experiments of Hart (e.g., 1986) indicate that the observed route to chaos is not similar to that predicted by the model of Pedlosky and Frenzen except perhaps in a small domain of parameter space.

The models mentioned above are fundamentally wave–mean flow interaction models. Although these systems are not truncated, initial conditions are chosen so that only a single wave is present in the initial data and the wave evolves and is limited in its amplitude by interaction solely with the mean zonal flow. Although such models are entirely self-consistent, they do not include any wave–wave interactions. It is natural to wonder whether such interactions might lead to vacillatory behavior of a type different to the Lorenz scenario and more like the observed transitions.

There have been a small number of investigations of wave–wave interactions in baroclinic flows already carried out (e.g., Hart, 1981; Mansbridge, 1984; Moroz and Holmes, 1984), but these have been at values of the dissipation sufficiently high so that only steady solutions are obtained. Thus, they have been unable to address the problem of vacillation. A more recent study by Mak (1986) uses a severe truncation of the quasi-geostrophic equations and suggests that wave–wave interaction may indeed be a mechanism to produce perpetual vacillation.

The present study was undertaken independently to also examine the role of wave–wave interaction in the dynamics of vacillation. The goal of the study was to produce an internally self-consistent, nontruncated model in which a pair of *unstable* waves interacted with one another as well as with the mean flow.

The model we choose is the classical Phillips model of baroclinic instability on the beta plane. Figure 1 shows the curve of marginal stability, in this case, β versus zonal wavenumber, k, in the inviscid limit. Note that for each value of β below the maximum critical value, there are two wavenumbers k_1 and k_2 which are marginally stable. The theory developed in this paper treats the evolution of two interacting waves, each of which is near the marginal waves k_1 and k_2. That is, the initial spectrum is restricted to just two slightly unstable waves. Although the resulting theory is consistent, one might wonder why the interval in k between k_1 and k_2, occupied by more unstable waves, can be ignored. Our fundamental attitude is that although it might seem natural to include such waves, we simply cannot within the limitations of the weakly nonlinear theory to be developed, and our overriding concern is to produce a consistent dynamical system with interacting waves rather than the fullest and most general theory. Furthermore, it is not difficult to imagine cases where the allowable zonal wavenumbers are quantized by a zonal periodicity condition such that k_1 and k_2 are the only allowable unstable modes, the intervening interval being denied by the quantization condition.

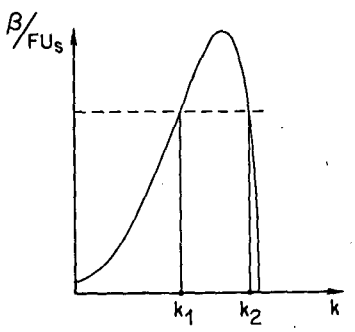

FIG. 1. A schematic rendering of the two-layer marginal stability curve in the β, k plane. β is the planetary vorticity gradient, U_s is the vertical shear, and $F^{1/2}$ is the ratio of the channel-width to the deformation radius. At values of β less than the maximum critical β, two zonal wavenumbers k_1 and k_2 are just marginally stable.

Thus our basic system will consist of the two waves, their nonlinearly generated harmonics ($k_1 \pm k_2$) and the evolving mean zonal flow.

Even this problem has some very subtle features which will become more evident in the subsequent technical development, but about which we wish to comment in these introductory remarks. It has been known for quite some time (Holopainen, 1961; Romea, 1977) that in the presence of very small Ekman layer dissipation, i.e., precisely the parameter range of interest for vacillation theories, the curve of marginal stability is shifted by an O(1) amount in the direction of *destabilization.* The parameter domain opened up by this order one shift contains only very weakly growing waves (growth rates of the order of the dissipation), but this is enough to seriously complicate the nonlinear problem. For, in this case, although the physically significant marginal curve is still the inviscid curve, any point on the marginal curve has an O(1) supercriticality with respect to the problem's first bifurcation point at the shifted marginal curve found by Holopainen. To avoid this technical difficulty, we adopt the following approach in the present paper. We alter the dissipation mechanism so that the dissipation of potential vorticity in each layer is directly proportional to the *potential* vorticity in each layer rather than the relative vorticity as in the case of Ekman dissipation. This is a device often used in theoretical models and in some ways has the advantage of representing a dissipation of the thermal as well as the momentum fields. The consequence of this substitution is striking. First of all, it renders the effect of dissipation on the marginal curve nonsingular, i.e., the marginal curve is shifted by only a small amount so that for small dissipation a perturbation theory hinged around the inviscid curve can be successfully carried out.

The other consequence of this change in the representation of dissipation turns out to be far more pro-

found for it will be shown below that potential vorticity dissipation, no matter how small its size, never allows for single-wave vacillation. That is, this apparently innocuous alteration of the dissipation mechanism completely expunges, for a single wave state, the Lorenzian chaotic behavior and the associated limit cycles. This is, of course, somewhat disturbing since the form of the dissipation is likely to be the least certain element of the dynamics. Again, this is another example of the structural instability of the original, baroclinic model of Pedlosky and Frenzen. This astonishingly sensitive reaction of the model can now be turned to conceptual advantage for it allows us to conclude that *the vacillation which is indeed found in the present model can be due only to wave–wave interaction.* Furthermore, the route to chaos found in this model is opposite to that found in the Lorenz model and in that of Pedlosky and Frenzen. Namely, in the present case chaotic behavior occurs as an end state when the dissipation is reduced with steady solutions giving way to periodic solutions which, in turn, are transformed to aperiodic solutions as dissipation is decreased.

In section 2 we describe the development of the amplitude equations in the present model and their relation to the Lorenz set. Section 3 forms a parenthesis in which a brief discussion is given of the role of interfacial friction in the f-plane model. It is shown there that for *weakly unstable disturbances,* the inclusion of interfacial friction leads to a form of dissipation indistinguishable from potential vorticity dissipation. In view of the remarks made above, this has profound and unexpected implications for models of f-plane vacillation.

In section 4 we briefly review Hart's (1981) analysis of steady mixed wave solutions which we find an invaluable guide for our numerical calculations in the vacillatory domain. Section 5 describes our numerical results illustrating the diverse parametric domains of behavior and the dependence on initial conditions. We also describe the linear stability of the mixed wave regime showing a narrow parameter range wherein the mixed steady solutions are rendered unstable by wave–wave interaction enforcing perpetual unsteadiness. The observed domain of vacillation in the model far exceeds the region of linear instability and is nearly coincident with the interval of allowed steady mixed solutions although in some cases we find vacillating solutions outside this interval.

Our overall conclusion is that the interaction between unstable waves provides a clear mechanism for vacillation, both periodic and chaotic. Moreover, it acts in cases, such as the one studied here, where wave–mean flow interaction alone leads to asymptotically steady solutions.

2. Derivation of the amplitude equations

We consider the basic flow to have only vertical shear, and we represent the dynamics of the perturbations with the use of the two-layer quasi-geostrophic model on the β-plane. The flow is contained in a channel of width L. The basic model is well known and readers are referred to Pedlosky (1970) for a derivation and discussion of the governing nondimensional potential vorticity equations. The equations for the perturbation geostrophic streamfunctions ϕ_n, $n = 1, 2$, are

$$\left(\frac{\partial}{\partial t}+U_n\frac{\partial}{\partial x}\right)[\nabla^2\phi_n+F(\phi_1-\phi_2)(-1)^n]+[\beta-F(U_1-U_2)(-1)^n]\frac{\partial\phi_n}{\partial x}$$
$$=-J[\phi_n,\nabla^2\phi_n+F(\phi_1-\phi_2)(-1)^n]-r[\nabla^2\phi_n+F(\phi_1-\phi_2)(-1)^n],\quad n=1,2. \tag{2.1}$$

The basic shear flow is U_n. The parameter F is the ratio of the channel width L to the deformation radius, $\sqrt{g'D}/f$, where D is the undisturbed depth of each layer. The parameter β is $\beta_* L^2/U$ where β_* is the dimensional planetary vorticity gradient and U is the scale for the horizontal velocity field.

The parameter r is introduced to parameterize the dissipation which in (2.1) is taken as linearly proportional to the perturbation potential vorticity.

For the inviscid normal mode problem, linear instability occurs when

$$\beta<F(U_1-U_2)\equiv\beta_M. \tag{2.2}$$

The critical curve in Fig. 1 is given by

$$\beta_I=\frac{(U_1-U_2)}{2F}a^2(4F^2-a^4)^{1/2} \tag{2.3}$$

where a^2 is square of the total wavenumber, i.e., $k^2 + l^2$.

Thus for each $\beta < \beta_M$ there are two values of a^2 for which a wavelike mode is just marginally stable, viz.:

$$a^2=2^{1/2}F\langle 1\pm\{1-\beta^2/[F^2(U_1-U_2)^2]\}^{1/2}\rangle^{1/2}. \tag{2.4}$$

The minus sign yields the long wave solution, a_1, to the left of β_M in Fig. 1, while the plus sign yields the short marginal wave, a_2, at the same value of β. For each a^2, the zonal wavenumber k^2 is given by

$$k=(a^2-l^2)^{1/2} \tag{2.5}$$

hence only those solutions to (2.4) with $a > l$ are physically meaningful where l is a multiple of π. Without exception in this paper, we will consider marginal waves which consist of the gravest cross-stream mode (the most unstable) for which $l = \pi$.

For each (β, a^2) pair, the phase speed of the marginal wave is given by

$$C=\frac{U_1+U_2}{2}-\frac{\beta(a^2+F)}{a^2(a^2+2F)} \tag{2.6}$$

which, with (2.3) may be used to show that the *long* wave always travels with a phase speed less than U_2

while the shorter wave always travels with a speed greater than U_2. Hence, the marginal pair consists of a short, fast wave and a long, slow wave (note that the slower wave lies *outside* the range of the basic velocity).

We shall examine the evolution of the wave pair for values of β slightly less than the critical value for a given shear. In the presence of the potential vorticity dissipation given in (2.1), the marginal curve is shifted only slightly from its inviscid value, namely

$$\beta_c = \beta_I - \frac{r^2}{k^2F^2}\frac{a^2(a^2+2F)}{2\beta_I}. \tag{2.7}$$

In distinction to the case with Ekman friction damping, $\beta_I \to \beta_c$ as $r \to 0$. Solutions to the problem will be sought for values of β such that

$$\beta = \beta_c - \Delta \tag{2.8}$$

where β_c is given by (2.7) and where

$$r = O(\Delta^{1/2}), \tag{2.9}$$

a parameter setting for which the dissipative time scale is of the same order as the e-folding development time for unstable baroclinic waves. We shall also allow k_1 and k_2 to shift slightly from the values given by (2.5) so that our actual parameter setting lies in some neighborhood near the critical points. For the purposes of ease of presentation, we defer for the moment the technical device used to allow a small change of k.

In the neighborhood of the critical points, ϕ_n will be a function of the advective time t and the slow, development time

$$T = \sigma t, \quad \sigma = O(\Delta^{1/2}) \tag{2.10a}$$

as discussed in Pedlosky (1970). Thus in (2.1)

$$\frac{\partial}{\partial t} \to \frac{\partial}{\partial t} + \sigma\frac{\partial}{\partial T}. \tag{2.10b}$$

The solution to (2.1) is sought in the form of an asymptotic series.

$$\phi_n = \epsilon(\phi_n^{(a)} + \epsilon\phi_n^{(1)} + \epsilon^2\phi_n^{(2)} + \cdots) \tag{2.11}$$

where ϵ is found to be $O(\Delta^{1/2})$.

The insertion of (2.8), (2.10b) and (2.11) into (2.1) yields a sequence of linear problems for the $\phi_n^{(j)}$ after terms of like order in ϵ are balanced.

The lowest order solution, at $O(\epsilon)$, yields

$$\phi_1^{(0)} = (A_1e^{i\theta_1} + A_2e^{i\theta_2})\sin ly + *$$

$$\phi_2^{(0)} = (\gamma_1A_1e^{i\theta_1} + \gamma_2A_2e^{i\theta_2})\sin ly + * \tag{2.12a,b}$$

where

$$\theta_m = k_m(x - c_mt), \quad m = 1, 2. \tag{2.13}$$

In (2.13), the subscript m labels each of the two marginal waves, i.e., solutions which satisfy (2.4), (2.5) and (2.6). As a convention, $m = 1$ will refer to the longer, slower wave. For each marginal wave, γ_m is the ratio between the amplitude in the lower and upper layers. It follows from the linear theory that γ_m, which is real, is given by

$$\gamma_m = \frac{a_m^2 + F}{F} - \frac{[\beta_I + F(U_1 - U_2)]}{F(U_1 - c_m)}. \tag{2.14}$$

The asterisks in (2.12a,b) denote the complex conjugate of the preceding term.

The next order problem for $\phi_n^{(1)}$ involves a forcing produced by the interaction between the two marginal waves. Some algebra yields

$$\left(\frac{\partial}{\partial t} + U_1\frac{\partial}{\partial x}\right)[\nabla^2\phi_1^{(1)} - F(\phi_1^{(1)} - \phi_2^{(1)})] + \frac{\partial q_1}{\partial y}\frac{\partial\phi_1^{(1)}}{\partial x} = \frac{\sigma}{\epsilon}\left[\left(\frac{\partial}{\partial T} + \frac{r}{\sigma}\right)\frac{A_1e^{i\theta_1}}{(U_1 - c_1)}\frac{\partial q_1}{\partial y} + \left(\frac{\partial}{\partial T} + \frac{r}{\sigma}\right)\frac{A_2e^{i\theta_2}}{(U_1 - c_2)}\frac{\partial q_1}{\partial y}\right]\sin ly$$

$$+ * + \frac{il}{2}\frac{\partial q_1}{\partial y}\frac{\sin 2ly}{(U_1 - c_1)(U_1 - c_2)}(c_2 - c_1)[(k_1 - k_2)A_1A_2e^{i(\theta_1+\theta_2)} + (k_1 + k_2)A_1A_2^*e^{i(\theta_1-\theta_2)}] + *. \tag{2.15a}$$

$$\left(\frac{\partial}{\partial t} + U_2\frac{\partial}{\partial x}\right)[\nabla^2\phi_2^{(1)} - F(\phi_2^{(1)} - \phi_1^{(1)})] + \frac{\partial q_2}{\partial y}\frac{\partial\phi_2^{(1)}}{\partial x} = \frac{\sigma}{\epsilon}\left[\left(\frac{\partial}{\partial T} + \frac{r}{\sigma}\right)\frac{\gamma_1A_1e^{i\theta_1}}{(U_2 - c_1)} + \left(\frac{\partial}{\partial T} + \frac{r}{\sigma}\right)\frac{\gamma_2A_2e^{i\theta_2}}{(U_2 - c_2)}\right]\frac{\partial q_2}{\partial y}\sin ly$$

$$+ * + \frac{il}{2}\frac{\partial q_2}{\partial y}\frac{\sin 2ly}{(U_2 - c_1)(U_2 - c_2)}(c_2 - c_1)\gamma_1\gamma_2[(k_1 - k_2)A_1A_2e^{i(\theta_1+\theta_2)} + (k_1 + k_2)A_1A_2^*e^{i(\theta_1-\theta_2)}]\sin 2ly + * \tag{2.15b}$$

where

$$\frac{\partial q_n}{\partial y} = \beta - (-1)^nF(U_1 - U_2). \tag{2.16}$$

The solution for $\phi_n^{(1)}$ consists of three parts. First, there are terms which represent a phase shift in each of the two marginal waves due to growth and dissipation. Second, there is, at this order, a correction to the mean flow in each layer. Both of these parts are familiar from the analysis of the single wave theory (e.g., Pedlosky, 1970). Now, however, the wave-wave interaction between the two marginal waves introduces into the solution, at this order, contributions with the sum and difference wave numbers and frequencies. A considerable amount of algebra allows us to write the solutions as

$$\phi_1(1) = A_1A_2R_1e^{i(\theta_1+\theta_2)}\sin 2ly + *$$

$$+ A_1A_2^*Q_1e^{i(\theta_1-\theta_2)}\sin 2ly + * + \Phi_1(y, T)$$

$$\phi_2^{(1)} = \frac{\sigma}{\epsilon}\left(\frac{\partial q_1/\partial y}{ik_1(U_1 - c_1)^2F}\right)\left(\frac{\partial A_1}{\partial T} + \frac{r}{\sigma}A_1\right)e^{i\theta_1}\sin ly + *$$

$$+\frac{\sigma}{\epsilon}\left(\frac{\partial q_1/\partial y}{ik_2(U_2-c_2)^2F}\right)\left(\frac{\partial A_2}{\partial T}+\frac{r}{\sigma}A_2\right)e^{i\theta_2}\sin ly+*$$
$$+\Phi_2(y,T)+A_1A_2R_2e^{i(\theta_1+\theta_2)}\sin 2ly+*$$
$$+A_1A_2^*Q_2e^{i(\theta_1-\theta_2)}\sin 2ly+*. \quad (2.17a,b)$$

where R_1, R_2, Q_1 and Q_2 are real constants given in Appendix A.

The forced wave solutions have zonal wavenumbers $k_{12}=k_1+k_2$ and $\alpha_{12}=k_1-k_2$ with associated frequencies $k_1c_1\pm k_2c_2$. The y wavenumber is $2l$. These solutions will be valid unless either of these sum and difference frequency–wavenumber pairs are themselves free solutions of the homogeneous part of (2.15a,b). The exceptional behavior does occur, but at only one value of β along the marginal curve. At that point alone, the forced solution is, in fact, a free solution and the problem must be rescaled by elevating the forced solution to a larger amplitude (ϵ instead of ϵ^2) and treating it, along with the marginal solutions, as the lowest order perturbation. Although this is an interesting circumstance, it is an isolated and uncharacteristic parameter one, and in this paper we shall simply avoid that problem by excluding that single value of β.

The solutions given by (2.17a,b) then combine with the two marginal waves to provide inhomogeneities for the $O(\epsilon^3)$ problem. As is usually the case, the inhomogeneities fall into two categories. One category is nonresonant and provides only an $O(\epsilon^3)$ correction to the $O(\epsilon)$ wave field and is inconsequential. There are two portions to the resonant inhomogeneities. One part is independent of x and t and the suppression of this resonance provides the equation describing how the potential vorticity fluxes in the wave field alter the mean flow.

After a good deal of algebra, it can be shown that

$$\Phi_1(y,T)=-\Phi_2(y,T)\equiv\Phi \quad (2.18)$$

where Φ satisfies

$$\left(\frac{\partial}{\partial T}+\frac{r}{\sigma}\right)\left[\frac{\partial^2\Phi}{\partial y^2}-2F\Phi\right]=\sum_{n=1}^{2}\frac{l\sin 2ly}{(U_1-c_n)^2}\frac{\partial q_1}{\partial y}\left[\frac{d}{dT}|A_n|^2+2\frac{r}{\sigma}|A_n|^2\right] \quad (2.19)$$

with

$$\partial\Phi/\partial y=0 \quad \text{at} \quad y=0,1. \quad (2.20)$$

Let

$$\frac{\partial^2\Phi}{\partial y^2}-2F\Phi=Q(T)l\sin 2ly\frac{\partial q_1}{\partial y}\frac{F^2}{\beta_1^2}, \quad (2.21)$$

then

$$\left(\frac{d}{dT}+\frac{r}{\sigma}\right)Q(T)=\sum_{n=1}^{2}\frac{(\beta/F)^2}{(U_1-c_n)^2}\left[\frac{d|A_n|^2}{dT}+2\frac{r}{\sigma}|A_n|^2\right] \quad (2.22)$$

while from (2.20) and (2.21)

$$\Phi=-Q(T)\frac{\partial q_1}{\partial y}\frac{l(F/\beta_1)^2}{(4l^2+2F)}\times\left[\sin 2ly-\frac{2^{1/2}l}{F^{1/2}}\frac{\sinh(2F)^{1/2}(y-1/2)}{\cosh(F/2)^{1/2}}\right]. \quad (2.23)$$

Note that the use of potential vorticity dissipation has allowed us to find the spatial structure of Φ separately from the determination of its time evolution as determined by (2.22)—a great simplification.

The remaining resonant forcing terms are wavelike where each has the horizontal structure of one of the two marginal waves. When each of the potentially secular terms are eliminated, two equations result, one for $A_1(T)$ and the other for $A_2(T)$. The details are laborious but standard (e.g., see Pedlosky, 1970), and we quote only the result, namely that A_1 and A_2 must be solutions of

$$\frac{d^2A_1}{dT^2}+2\mu\frac{dA_1}{dT}-X_1A_1+A_1QY_1+A_1|A_2|^2Z_{12}=0$$
$$\frac{d^2A_2}{dT^2}+2\mu\frac{dA_2}{dT}-X_2A_2+A_2QY_2+A_2|A_1|^2Z_{21}=0. \quad (2.24a,b)$$

In obtaining (2.24a,b) we have chosen the time scale σ (see 2.10a) such that

$$\sigma=\Delta^{1/2}(\beta_1/F)^{1/2}$$
$$\epsilon=(\Delta\beta/F^3)^{1/2}$$

and have made use of (2.21) and (2.23). The dissipation parameter $\mu\equiv r/\sigma$. The constants X_n, Y_n, Z_{mn} are real and given in Appendix B. The analytical expressions are very complex but the interpretation of (2.24a,b) is very straightforward. The first three terms in each equation represent the linear theory for each wave and, if X_n is greater than zero, then A_n will grow exponentially according to linear theory. The fourth term in each equation represents the wave–mean flow interaction where the parameter Y_n, given by (B4), measures the strength of that interaction for each wave. For all points along the marginal curve, the Y_n are positive (see Fig. 2a) so that the wave–mean flow interaction is always stabilizing.

The last term in (2.24a,b) represents the wave–wave interaction. When each $O(\epsilon)$ fundamental wave with phase θ_n interacts with the $O(\epsilon^2)$ forced waves with phases $\theta_1\pm\theta_2$, an $O(\epsilon^3)$ forcing term with the same frequency and wavenumber as one of the two fundamental waves occurs. This leads to the coupling term in (2.24a,b) between the two waves. If the Z_{mn} are negative, the wave–wave interaction consists of each wave *destabilizing* the other. Were they both positive, the waves would act as mutual stabilizers. If one is negative and the other positive, a strong asymmetry occurs in the wave–wave transfer.

Figure 2b shows the calculated values of Z_{mn} as a

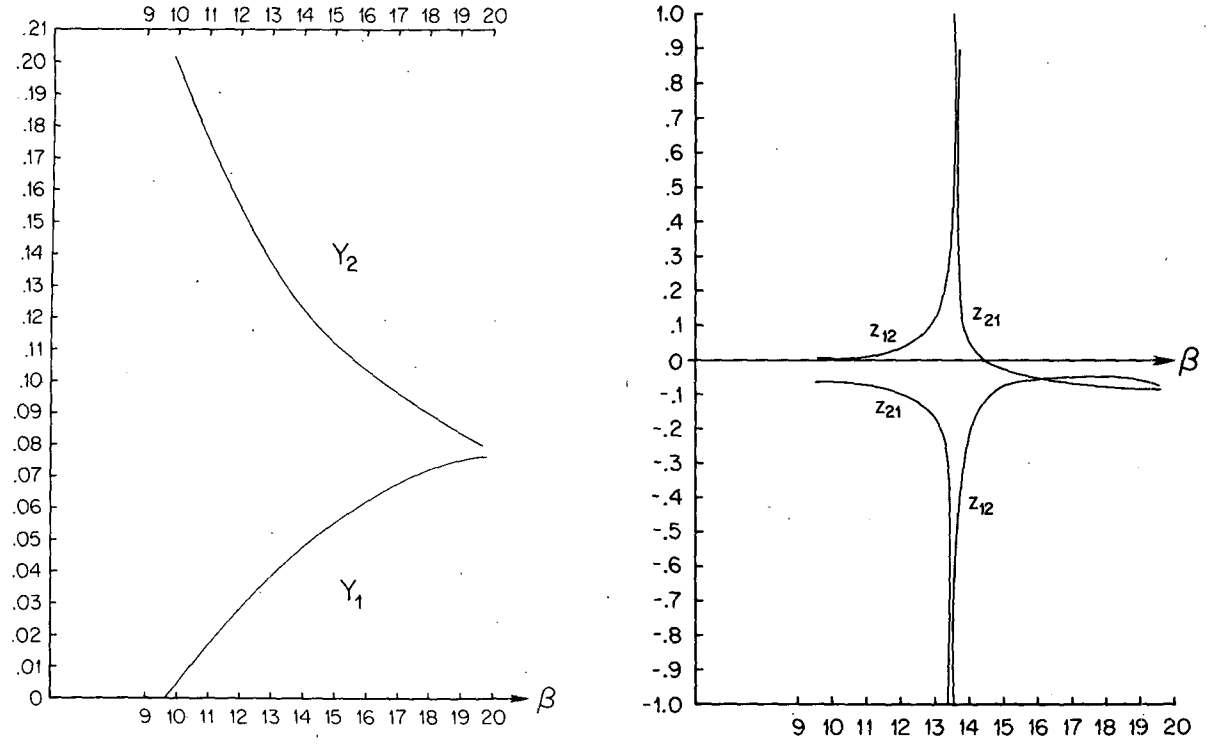

FIG. 2. (a) The wave–mean flow interaction coefficients as a function of β in the range for which $k_1^2 > 0$ for $F = 2\pi^2$. (b) The wave–wave interaction coefficients for the same case as in (a).

function of β along the neutral curve for the case $F = 2\pi^2$, $U_1 - U_2 = 1$. For this case the maximum β is $2\pi^2$ or about 19.74. The minimum value of β for which k_1 is real, occurs when $\beta = 9.556$. Note that, as Fig. 2b shows, both Z_{12} and Z_{21} are negative for $\beta \gtrsim 14.3$ below which Z_{21} changes sign. The singularity in the calculated Z_{mn} at about $\beta = \beta_0 \sim 13.5$ occurs at that single point, where one of the forced solutions happens to be also a free solution. As remarked earlier, in the neighborhood of this point, the problem must be recast and the $O(\epsilon)$ perturbation must include the formerly forced solution in the fundamental perturbation field. We will avoid that complexity entirely by not allowing β to take on that particular value which renders Z_{mn} infinite.

For the most part we shall focus attention in the range $\beta_{\max} > \beta > \beta_0$ where both Z_{mn} are negative. Since this is the range contiguous to the maximum critical β (or the minimum critical shear) for instability, it is of obvious interest. We shall, however, comment below on the behavior of (2.24a,b) for $\beta < \beta_0$.

Define

$$\alpha_n = \frac{2(\beta_1/F)^2}{(U_1 - c_n)^2}. \tag{2.25}$$

Then the final set of amplitude equations consist of (2.24a,b) along with (2.22) rewritten as

$$\left(\frac{d}{dT} + \mu\right) Q = \sum_{n=1}^{2} \frac{\alpha_n}{2}\left[\frac{d|A_n|^2}{dT} + 2\mu|A_n|^2\right]. \tag{2.26}$$

If the form of (2.24a,b) is examined carefully, an apparently innocuous difference is evident between the linear dissipation term, $2\mu(dA_n/dT)$, in the present problem and its form in the f-plane, Ekman dissipation problem (Pedlosky and Frenzen, 1980) in which the dissipation term goes like $\frac{1}{2}\mu(dA/dT)$. In both problems the frictional term in the nonlinear forcing of the mean field goes like $2\mu|A_n|^2$. This small difference has a dramatic effect which can be appreciated by considering the relation of each problem to the Lorenz equations (Lorenz, 1963)

$$\left.\begin{aligned} \frac{dy}{d\tau} &= \sigma(x - y) \\ \frac{dx}{d\tau} &= Ry - x - yz \\ \frac{dz}{d\tau} &= xy - bz \end{aligned}\right\}. \tag{2.27a,b,c}$$

Let us make the following transformation of the Lorenz set. Let

$$\left.\begin{aligned} y &= y_0\tilde{A} \\ z &= z_0\tilde{Q} \\ \tau &= sT \end{aligned}\right\}, \tag{2.28}$$

then $\tilde{A}$ and $\tilde{Q}$ satisfy

$$\frac{d^2\tilde{A}}{dT^2}+(\sigma+1)s\frac{d\tilde{A}}{dT}-\sigma(R-1)s^2\tilde{A}+\sigma s^2 z_0\tilde{Q}\tilde{A}=0$$

$$\frac{d\tilde{Q}}{dT}+bs\tilde{Q}=\frac{1}{2}\frac{y_0^2}{z_0}\sigma\left[\frac{d\tilde{A}^2}{dT}+2\sigma s\tilde{A}^2\right]. \quad (2.29a,b)$$

Consider now the case where in the wave problem (2.24a,b) only one wave is present in the initial data; for example, consider the solution which has $A_2 = 0$ and only $A_1 \neq 0$. Then the equation for A_1 can be put exactly in the form of the Lorenz set with the proper choices of σ, s, b, z_0, y_0 and R_0. The amplitude scales y_0 and z_0 are inconsequential. The crucial fact is that the equivalence of the single wave form of (2.24a,b) and the Lorenz set requires $\sigma = 1$ and $b = 1$ independent of any other parameter. On the other hand, when Ekman friction is responsible for the dissipation, it is easy to show that the equivalence requires $\sigma = 2$ while b is a number less than 1. The importance of this follows from the fact that when $\sigma = b = 1$, the *steady* solutions of the Lorenz equations are stable for all values of R (i.e. μ) to both infinitesimal and finite perturbations. All solutions tend with time to the steady solutions and vacillating behavior, both periodic and chaotic, is absent. This can be verified by direct numerical integrations of the Lorenz set and the analysis of the stability of the steady solutions.

Thus, for all μ, no matter how small, *the introduction of dissipation proportional to the potential vorticity rather than the relative vorticity, completely expunges the phenomenon of wave–mean flow vacillation.* It was noted in Pedlosky and Frenzen (1980) that the wave–mean flow dynamics was very sensitive to the value of dissipation. It now appears that the amplitude dynamics is also exquisitely sensitive to the *type* of dissipation as well as just the overall dissipation time scale. Since the particular representation of dissipation is one of the least certain aspects of atmospheric and oceanographic modeling, this is a disturbing result and it gives greater urgency to our goals of examining whether the two-wave system which contains wave–wave interaction can restore the possibility of vacillation which potential vorticity dissipation excludes from the more simple wave–mean flow dynamics.

To some extent we have stumbled onto this result. Recall, that we originally chose a representation of the dissipation of this form only to avoid a technical difficulty present in the O(1) linear problem, i.e., the singular shift of the marginal curve when the β-effect interacts with Ekman damping. It is, however, easy to return to the original f-plane model of Pedlosky and Frenzen (1980) where that difficulty does not occur. It is a simple matter in that case to show that, if dissipation is similarly parameterized in terms of potential vorticity, the resulting amplitude equations have their Lorenz equivalence also requiring $\sigma = b = 1$. Thus, the suppression of the vacillating behavior for wave–mean flow interaction is due entirely to the *form* of the dissipation and not its relation to the β-effect. Once again the structural instability of the wave–mean flow problem has been exposed.

Before proceeding to the wave–wave problem as described by (2.24) and (2.26), we will make a short parenthesis in section 3 to discuss the implications of the result described above for the f-plane problem including interfacial friction. Readers who would prefer to proceed directly to the two-wave problem may turn directly to section 4.

3. Wave–mean flow interaction on the f-plane: Interfacial friction

The earliest models of finite amplitude baroclinic instability which included Ekman dissipation were for the two-layer model (Pedlosky, 1970) in which the effect of the Ekman layers was included only at the rigid horizontal boundaries. The effect of interfacial Ekman layers was purposely ignored for two reasons. First, simply to reduce the amount of algebra and second, and more importantly, to try to mimic better the continuous model in which, of course, internal dissipation of the Ekman type is not possible. Thus, it is fair to characterize the earliest f-plane, two-layer models as crude attempts to model a continuous system in which dissipation acts only on the boundaries of the fluid.

However, it then becomes apt to ask how well such a model will do in representing the physically realizable two-layer model studied in the laboratory, e.g., the very careful experiments of Hart (1972). In such a case, interfacial friction must be included to represent the dissipative mechanism at the interface of the two layers. Using standard boundary layer analysis, one can show that (Hart, 1972) the form of the potential vorticity equation in this case is simply

$$\frac{d}{dt}q_n=-r\left[\zeta_n-\frac{(-1)^n}{2}(\zeta_1-\zeta_2)\right], \quad n=1,2 \quad (3.1)$$

where q_n is the potential vorticity in each layer and ζ_n is the relative vorticity in each layer.

For the f-plane model, instability occurs for a plane wave, with total wavenumber, a, when (Pedlosky, 1970)

$$a^2=2F, \quad (3.2)$$

and this will be true for the horizontal plan form of the entire *wave* field in the asymptotic theory. However, since $\zeta_n = \nabla^2\phi_n$, it follows that for such a wave

$$\zeta_n-\frac{(-1)^n}{2}(\zeta_1-\zeta_2)=\nabla^2\phi_n+\frac{(-1)^n}{2}a^2(\phi_1-\phi_2)$$

$$=\nabla^2\phi_n+(-1)^nF(\phi_1-\phi_2)$$

$$=q_n. \quad (3.3)$$

Thus on the f-plane, for a weakly unstable wave, the

effect of including interfacial friction in the two-layer model is equivalent to assuming that the dissipation of potential vorticity is proportional to the potential vorticity itself, as in section 2. The implications are striking if the arguments of section 2 are now applied. Although it has long been thought that adding interfacial friction would do nothing more than serve to increase the effective value of μ, in fact the structural change in the governing equations as manifested by the change in the Lorenz equivalent of σ, will completely alter the behavior of finite amplitude waves, at least in weakly nonlinear theory, by expunging the vacillation springing from wave–mean flow interaction. Paradoxically, the two-layer, wave–mean flow interaction model without Ekman friction at the interface is a better model of the continuous Eady model than the actual two-layer physical system in which Hart has found vacillation and chaotic behavior. Indeed, calculations of the Eady model, not given here, yield a Lorenz equivalent σ of about 1.44 and $b < 1$ for which vacillation does indeed exist. This astonishing turn of events, namely, the unexpectedly immense sensitivity of the finite amplitude dynamics to the form of the dissipation, suggests further examination of the *f*-plane problem. Such work is underway in cooperation with P. Klein and will be reported upon separately. We have felt it important though to report on this development which has come to light unexpectedly during our study of the wave–wave interaction problem, to whose discussion we now return in Section 4.

4. The steady mixed wave regime

Before proceeding to the discussion of time-dependent wave states, it is useful to consider the nature of the possible steady solutions, in particular, to discover the parametric requirements for *mixed* wave states in which both waves may be present simultaneously. Although the basic physical models are quite different, it turns out that the discussion of the steady solutions in our case parallels Hart's (1981) analysis in which he described the wave–wave interaction of two modes on the *f*-plane for $r = O(1)$ for which value of r the governing amplitude equations are each first order. To ease a comparison with Hart's treatment, we introduce the following variables

$$\left.\begin{aligned} P &= Q - \sum_{n=1}^{2} \alpha_n |A_n|^2 \\ d_1 &= \frac{\alpha_2}{\alpha_1} + \frac{Z_{12}}{\alpha_1 Y_1} \\ d_2 &= \frac{\alpha_1}{\alpha_2} + \frac{Z_{21}}{\alpha_2 Y_2} \end{aligned}\right\} \quad (4.1a,b,c)$$

in terms of which (2.24a,b) and (2.26) may be rewritten as

$$\left.\begin{aligned} &\frac{d^2A_1}{dT^2} + 2\mu\frac{dA_1}{dT} - X_1A_1 + A_1\alpha_1Y_1[|A_1|^2 + d_1|A_2|^2] \\ &\qquad + A_1PY_1 = 0 \\ &\frac{d^2A_2}{dT^2} + 2\mu\frac{dA_2}{dT} - X_2A_2 + A_2\alpha_2Y_2[|A_2|^2 + d_2|A_1|^2] \\ &\qquad + A_2PY_2 = 0 \\ &\frac{dP}{dt} + \mu P = -\sum_{n=1}^{2} \frac{\alpha_n}{2}\frac{d}{dt}|A_n|^2 \end{aligned}\right\} \quad (4.2a,b,c)$$

Steady solutions of (4.2a,b,c) fall into two classes; either single wave solutions ($A_1 \neq 0$, $A_2 = 0$ or vice versa) or mixed wave solutions in which both A_1 and A_2 are different from zero. Define $\hat{A}_n$ as the "stand alone" amplitude for the single-wave solution. It follows from (4.2a,b,c) that for the steady single-wave solution, either

$$|\hat{A}_1|^2 = X_1/\alpha_1Y_1, \quad |A_2|^2 = 0 \quad (4.3)$$

or

$$|\hat{A}_2|^2 = X_2/\alpha_2Y_2, \quad |A_1|^2 = 0, \quad (4.4)$$

and these solutions are possible (though not necessarily stable) for all values of

$$S = \frac{X_2}{X_1}\frac{\alpha_1Y_1}{\alpha_2Y_2} = \frac{|\hat{A}_2|^2}{|\hat{A}_1|^2}. \quad (4.5)$$

Mixed, steady wave solutions are also possible. Solving (4.2a,b,c) in the case when both A_1 and A_2 are different from zero, yields

$$|A_1|^2 = \frac{X_1}{\alpha_1Y_1}(1 - d_1S)/(1 - d_1d_2)$$

$$|A_2|^2 = \frac{X_2}{\alpha_2Y_2}(S - d_2)/(1 - d_1d_2). \quad (4.6a,b)$$

For the mixed wave solution to be possible $d_1d_2 \neq 1$ and reference to (4.1b,c) shows that this will be true only due to $Z_{mn} \neq 0$, i.e., only as a consequence of wave–wave interaction. Direct calculation of d_1 and d_2 along the marginal curve (see Fig. 3) shows that not only is $d_1d_2 \neq 1$ but that $d_1d_2 < 1$. In this case, as Hart demonstrates, mixed-wave, steady solutions are possible in the parameter range

$$d_2 < S < d_1^{-1} \quad (4.7)$$

and they will certainly be linearly stable when μ is large enough for each of (4.2a,b,c) to be approximated by its first order form. We shall discuss the linear instability of the steady solutions for arbitrary μ below, but for the present, the important result is the description of an interval in parameter space, given by (4.7) in which it is natural to search for mixed steady, and by extension, mixed vacillating solutions.

Note that as $S \to d_2$, $|A_2|^2 \to 0$ and $|A_1|^2 \to |\hat{A}_1|^2$ while as $S \to d_1^{-1}$, $|A_1|^2 \to 0$ and $|A_2|^2 \to |\hat{A}_2|^2$ so that there is continuity across the boundaries of the steady solutions.

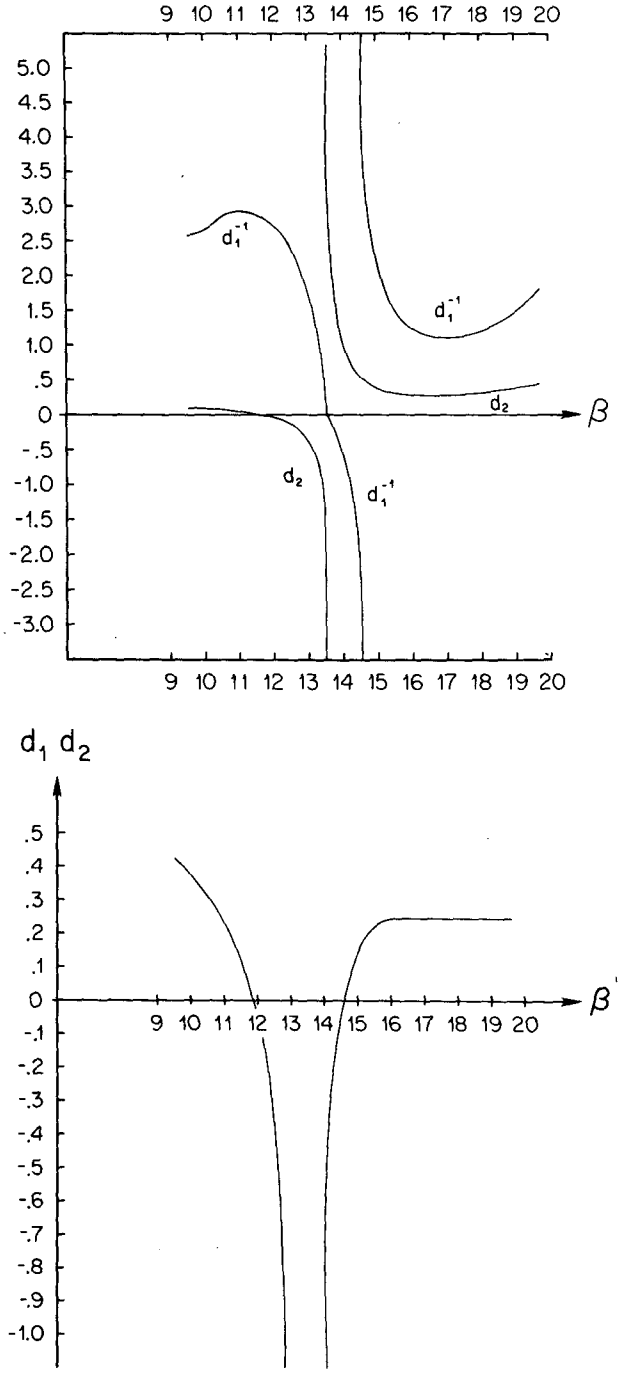

FIG. 3. (a) The coefficients d_1^{-1} and d_2 for $F = 2\pi^2$ as a function of β. Note that $d_2 < d_1^{-1}$. (b) The factor $d_1 d_2$. Note that $d_2 d_1 < 1$.

Of course, it remains to be seen whether the interval (4.7) holds as the domain for mixed time-dependent solutions but, anticipating our results of section 5, we find that roughly it is, so that it provides excellent guidance for the search in parameter space.

For given values of β and F, the coefficients X_n, α_n, Y_n, Z_{mn} and, thus, d_n are fixed. Thus, S is the only variable for fixed β aside from the dissipation μ. Here S may be arbitrarily placed in the interval (d_2, d_1^{-1}) by simply altering the relative linear growth rates of the two waves, i.e., X_2/X_1. This can be achieved for a fixed Δ by independently altering, by an $O(\Delta)$ amount, the wavenumbers of the two marginal waves as described in Appendix B [see especially Eqs. (B7) and (B8), and Fig. 4]. This device lets us scan the entire range in S in a search for vacillating solutions.

We would also like to point out the difference between our results and those of Hart's for the f-plane case and Mansbridge's for the β-plane case [for which Ekman dissipation was taken to be O(1)]. In each of those calculations $d_1 d_2$ was greater than one and so implies a hysteresis behavior between two single wave states rather than mixed wave states. The different is clearly related to the differing structures of the waves and their interactions in these three separate parameter regimes.

Even for the steady case, the time dependence of the total solution is not trivial since $c_1 \neq c_2$, i.e., the waves, although separately steady, move past each other so that at any fixed point the observed wave disturbance amplitude will oscillate with both frequencies $k_1 c_1$ and $k_2 c_2$. Such an oscillation must be distinguished, however, from the case where each of A_1 and A_2 separately pulsate on a long time scale. The difference is especially important when the pulsation is aperiodic.

5. Numerical results

The system (2.24a,b), (2.26) which governs the behavior of the two-wave dynamics was integrated numerically at several values of β. For each value of β, i.e., for each setting below the maximum critical β for instability, the relative growth rates of the two waves were altered by small adjustments to the wavenumber in order to allow the parameter S, defined by (4.5), to span an interval which included the range (4.7) in which mixed steady solutions (4.6a,b) are possible. We quickly discovered that the range $d_2 < S < d_1^{-1}$ was a good rough indicator of the domain of mixed solutions of all types, vacillatory as well as steady, although there

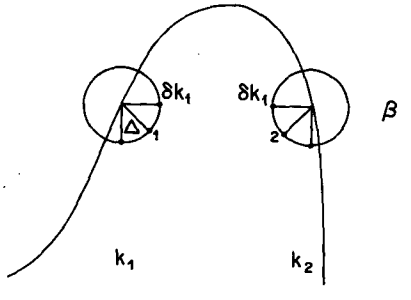

FIG. 4. A schematic shows the neighborhoods in the β, k plane in which slightly unstable waves occur. β is $O(\Delta)$ less than its critical value while k_1 and k_2 can both be simultaneously shifted with respect to their marginal values.

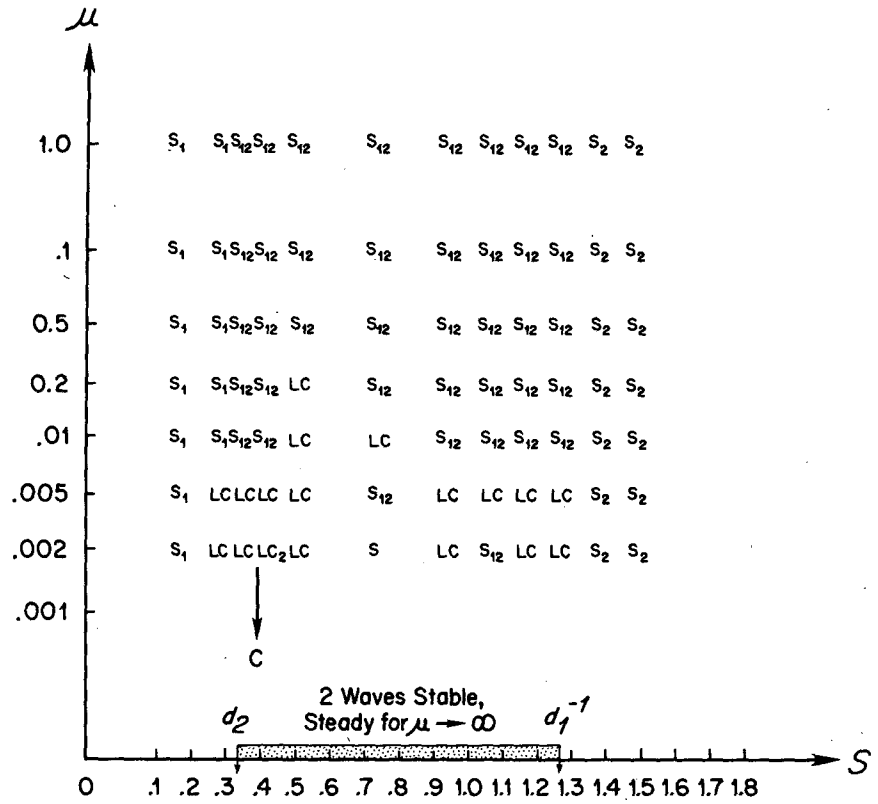

FIG. 5. A map of the S, μ parameter space for $\beta = 15.79$ and $F = 2\pi^2$, $U_s = 1$ (i.e., $\beta/FU_s = 0.8$). Points labeled S_1, S_2, S_{12} show where steady solutions comprised of only wave one, only wave two, or a mixture, respectively, are found. Points marked LC represent mixed, periodic wave vacillation, LC_2 represents a periodic solution of doubled period. The arrow pointing to C describes the transition to chaotic behavior described in the text. The bar at the bottom shows the interval $d_2 \leq S \leq d_1^{-1}$ where the steady mixed solutions are possible.

are examples in which mixed-wave time-dependent solutions occur somewhat outside the range given by (4.7). Time dependence slightly enlarges the mixed wave domain. Calculations presented in section 6 demonstrate that the steady solutions are linearly stable except for very small μ within a very narrow range of S [much smaller than (d_2, d_1^{-1})]. Thus as in the wave–mean flow vacillations described by Pedlosky and Frenzen (1980), finite amplitude vacillation will be seen to occur in domains where the steady solutions are linearly stable but with an obviously finite attractor basin, which does not include the initial data. The initial data for all the examples to be described have Q equal to zero, i.e., no initial correction to the zonal flow; and A_n and (dA_n/dt) are either zero or one.

Most of our attention has been focussed on the region in which both Z_{12} and Z_{21} are negative, i.e., for $\beta \geq 14.31$, for $F = 2\pi^2(19.739)$. A typical example of our results is shown in Fig. 5, which is a map of results of the calculations. The map shows the μ and S domain in which the calculations were done. Each point is labeled according to the asymptotic character of the solutions. It must be understood that if only a single wave is present in the initial data, only that wave exists in the solution, and it must be ultimately steady. Thus, Fig. 5 implicitly assumes mixed initial data. Usually both A_1 and A_2 were unity at the initial instant. Points labeled S_n ($n = 1$ or 2) denote steady solutions in which wave n (1 or 2) is the *only* wave ultimately remaining. Points marked S_{12} denote a steady final wave state in which both waves were present. Points labeled LC refer to asymptotic states in which both wave amplitudes pulsate periodically. Not shown on the map in detail, but described below, is a fine survey in μ along the line $S = 0.38390$ where, for quite small μ, aperiodic mixed wave vacillation is observed.

Figure 6 shows a typical evolution sequence for high μ, e.g., $\mu = 1$, for $S < d_2$. As predicted, wave 1 equilibrates to its stand-alone value $\hat{A}_1$ given by (4.3) while $A_2 \to 0$. Figure 7 shows a similar evolution to a mixed-wave regime for S within the range (d_2, d_1^{-1}) for $\mu = 1$.

Figure 8 shows a portion of the mixed-wave periodic vacillation at $\mu = 0.002$ and $S = 0.27392 < d_2$, i.e.,

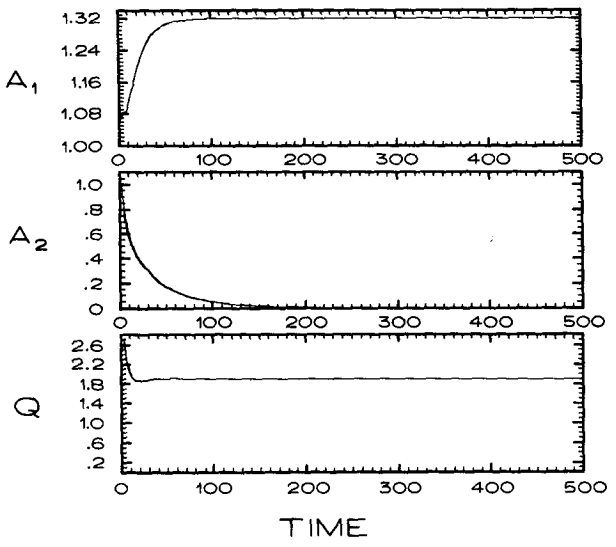

FIG. 6. The amplitude evolution for $\beta = 15.79$, $F = 2\pi^2$, $\mu = 1$ showing the evolution to a single wave solution. S lies outside the (d_2, d_1^{-1}) interval.

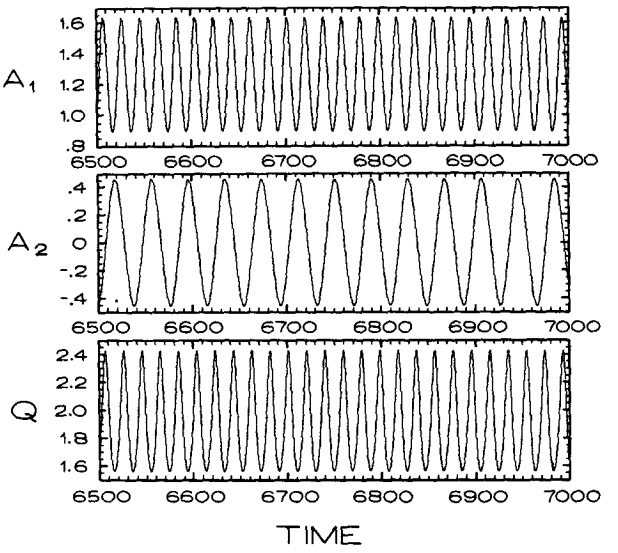

FIG. 8. For the same values of β and F as in Figs. 6 and 7, but for $\mu = 0.002$ and $S = 0.27392$, a mixed, periodic solution obtains. Note that A_1 is always positive while A_2 passes through zero.

outside the interval of steady mixed-wave solutions. Since this vacillation occurs at such small values of μ for which the dissipation time scale, μ^{-1}, is 500 in these units (about 500 linear e-folding times for the unstable waves), we decided it would be prudent to continue the calculation for several times the dissipation time scale. It should thus be noted that the periodic solution persists at least to $T = 7 \times 10^3$ which is about 14 times the dissipation time scale. Note that in this solution A_1 is always positive and considerably greater than A_2, which changes sign during the vacillation. Recall that this vacillation exists in addition to the nontrivial time dependence possessed by the pair of waves due to the fact that $c_1 \neq c_2$. A similar oscillation, not shown, also occurs at $S = 0.3179$, i.e., within the interval (d_2, d_1^{-1}).

Figure 9 shows an example, at $S = 0.4938$, where both A_1 and A_2 pulsate without change of sign. Figure 10, on the other hand, shows that at $S = 0.9338$ both amplitudes pass through zero during their vacillation cycle. Hence each of the possible combinations of vacillation is possible. We have been unable, even for small μ, to construct a theory to determine a priori the nature

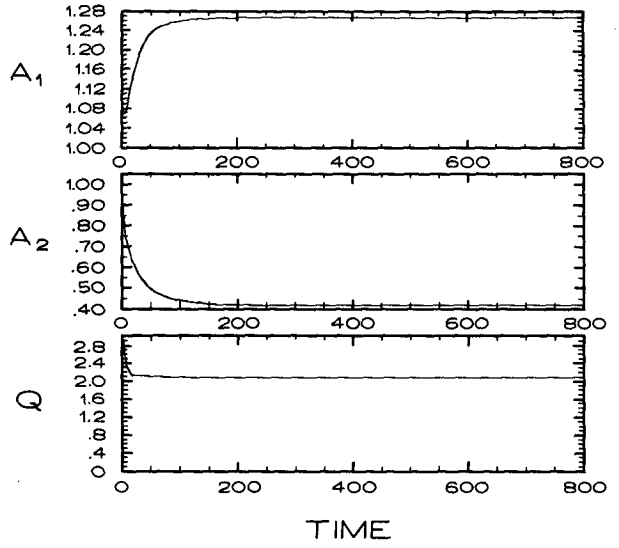

FIG. 7. As in Fig. 6 but S lies within (d_2, d_1^{-1}), and a mixed steady solution is obtained. Note that A_2 is asymptotic to $A_2 \sim 0.4$.

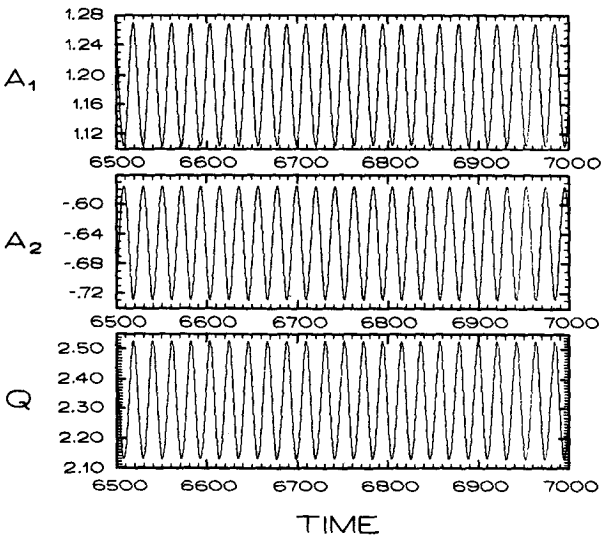

FIG. 9. As in Fig. 8 but $S = 0.49387$. Both A_1 and A_2 vacillate periodically without change of sign.

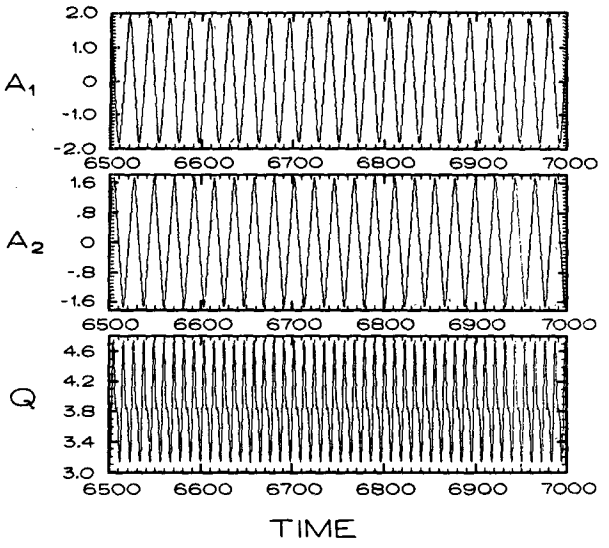

FIG. 10. As in Fig. 9 but $S = 0.9379$. Both A_1 and A_2 vacillate periodically and both pass through zero.

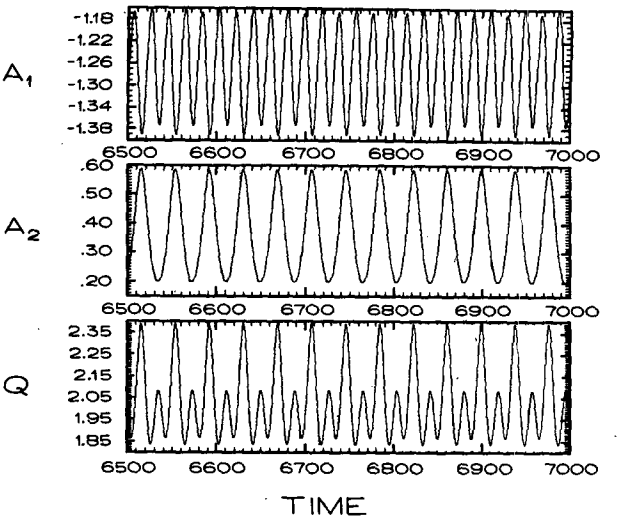

FIG. 11. As in Fig. 10 but $S = 0.3839$. Note that A_1 and Q oscillated with a doubled period.

of the vacillation cycle for each amplitude as a function of S that parallels the theory for single wave limit cycles (Pedlosky, 1972) and so our results are limited to our numerical calculations.

Nor in lowering μ could we find chaotic behavior or period doubling in any interval *between* these periodic solutions and the steady solutions, in distinction to the wave–mean flow model of Pedlosky and Frenzen (1980).

We chose one value of S, $S = 0.38390$, for a fine-scale investigation of the μ line for small μ. The qualitative results are shown in Table 1. There is no completely uniform progression in type as μ is decreased, but there is a distinct qualitative change. As μ is decreased, we observe a transition from the type of periodic solution shown in Fig. 10 to an oscillation shown in Fig. 11, referred to in the table as LC_2, where *one* of the waves, in this case A_1, suffers a period-doubling while A_2 appears to maintain its period. This behavior is common but not realized uniformly as μ decreases, for at smaller μ the original limit cycle (Fig. 10) reappears as shown in Table 1. It is interesting to note that the period of A_2 is nearly precisely double that of A_1 so the period-doubling of A_1 locks high amplitude levels of A_1 with crests of A_2 and low amplitudes of A_1 to troughs of A_2.

At much smaller values of μ, as in the case shown in Fig. 12, the solution is chaotic for A_1, A_2 and Q. Again, the solution has been run until $T = 7000$. How-

TABLE 1. Shows the solution behavior at $S = 0.3839$ for $0.0002 \leq \mu \leq 0.0025$. The notation is as in Fig. 5. Note the progression from periodic to aperiodic solutions as μ is decreased. For some intermediate values of μ, a double period solution is found.

$\mu = 0.0002$	C
0.0005	C
0.001	LC
0.0012	LC
0.0015	C
0.0018	LC
0.00185	LC_2
0.00186	LC
0.00188	LC_2
0.00189	LC
0.0019	LC_2
0.00195	LC
0.00198	LC
0.002	LC_2
0.00205	LC
0.0021	LC
0.0025	LC

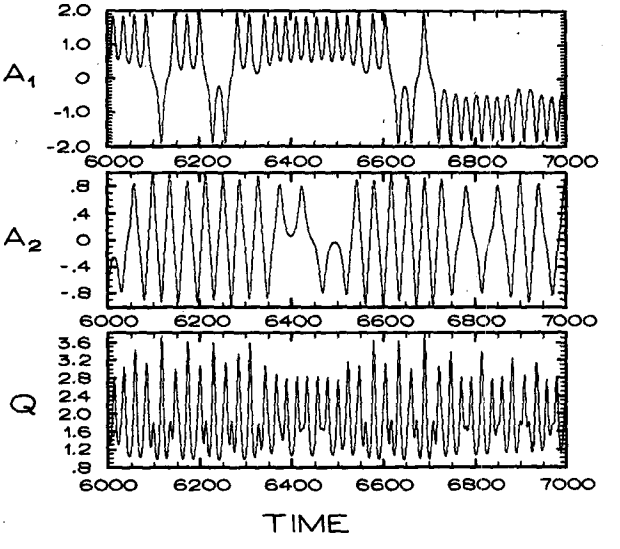

FIG. 12. The chaotic solution at $\mu = 0.0005$, $S = 0.3839$.

ever, in this case, this represents only 3.5 dissipation time scales, and it is conceivable that the solution might ultimately settle into a more regular state. The form of the solution is nevertheless unlike those of any preperiodic transition interval at higher μ, and we are far from the larger μ steady solutions. We therefore, at least tentatively, identify the progression with decreasing μ as being from steady to periodic to chaotic behavior with some hint of period doubling but no evidence of the complete Feigenbaum sequence present in the study of Pedlosky and Frenzen (1980). We emphasize again that this chaotic behavior, as well as the limit cycle behavior at larger μ, is due solely to the presence of wave–wave interaction, without which in this model, wave–mean flow interaction would yield ultimately only a steady wave. Although the detailed physics of the model is quite different from those of the experiments of Hart (1986), we suggest that wave–wave interaction can lead to the same qualitative route to chaos found in the experiments. Furthermore, it appears, at least in this study, that the wave interaction mechanism may be a more robust mechanism for chaotic behavior than wave–mean flow interaction.

6. Linear stability of steady solutions

Although the finite-amplitude dynamics is not very sensitive to stability of the steady wave solutions with respect to small perturbations, there are some interesting aspects to this problem to which we would like to refer. Again, the key differences are related to the wave–wave interaction mechanism.

We denote the steady mixed wave solutions as $\bar{A}_n$ and the small perturbations as $a_n(T)$ so that

$$A_n = \bar{A}_n + a_n \tag{6.1}$$

where $\bar{A}_n$ is given by (4.6a,b). Furthermore, we may write

$$a_n = \tilde{a}_n e^{\sigma T}. \tag{6.2}$$

Similarly, we write

$$Q_n = \bar{Q}_n + q_n e^{\sigma T}. \tag{6.3}$$

If these forms are inserted in (2.24) and (2.26), we obtain the following equations for $\tilde{a}_n$:

$$\tilde{a}_1\left[\sigma^2 + 2\mu\sigma + 2\alpha_1 Y_1 \bar{A}_1^2 - \frac{\alpha_1\sigma}{\sigma+\mu} Y_1 \bar{A}_1^2\right] + \tilde{a}_2\left[2\alpha_1 Y_1 d_1 - \alpha_2 Y_1 \frac{\alpha}{\sigma+\mu}\right]\bar{A}_1\bar{A}_2 = 0.$$

$$\tilde{a}_2\left[\sigma^2 + 2\mu\sigma + 2\alpha_2 Y_2 \bar{A}_2^2 - \frac{\alpha_2\sigma}{\sigma+\mu} Y_2 \bar{A}_2^2\right] + \tilde{a}_1\left[2\alpha_2 Y_2 d_2 - \alpha_1 Y_2 \frac{\alpha}{\sigma+\mu}\right]\bar{A}_1\bar{A}_2 = 0. \tag{6.4a,b}$$

The characteristic equation for σ, obtained by setting the determinant of (6.4a,b) to zero, determines the growth rate, σ, of the perturbations. The resulting equation is fifth order in σ, and we have solved it numerically. Some results are shown in Table 2. First, we note that the steady solutions are stable for small μ for nearly all S in the interval (d_2, d_1^{-1}), where the mixed solution is possible. This is quite different than the single wave–mean flow case. In that case, the steady solutions became unstable for small μ through a Hopf bifurcation whenever $k > \sqrt{3}l$.

As $\mu \to 0$, the equation for σ reduces to a quantic

$$\sigma^4 + \sigma^2(\alpha_1 Y_1 \bar{A}_1^2 + \alpha_2 Y_2 \bar{A}_2^2) - 2(Z_{12}\alpha_1 Y_2 + Z_{21}\alpha_2 Y_1) \times \bar{A}_1^2 \bar{A}_2^2 - 4Z_{12}Z_{21}\bar{A}_1^2\bar{A}_2^2 = 0. \tag{6.5}$$

Note that if the Z_{mn} are zero, i.e., no wave–wave interaction, σ^2 would be negative and σ purely imaginary as $\mu \to 0$. In that case, the growth rate of any instability becomes $O(\mu)$ as μ is increased from zero. However, the presence of wave–wave interaction alters this behavior and, in a narrow range of S, an inviscid instability of the steady mixed waves is assured. Note that the steady, single-wave solutions are also unstable in this interval, so that for at least this slender range of S, all solutions must remain time dependent.

A comparison of Fig. 5 with Table 1 shows that at a fixed value of S, in this case, $S = 0.49387$, the transition from stable to unstable steady solutions occurs

TABLE 2. (a) The most unstable root of (5.4) as a function of S for $\mu = 0$. Note that σ is only positive for $d_2 < S < d_1^{-1}$ within a very narrow range of S. (b) σ as a function of μ showing the linear stabilization of the steady solutions for $\mu \geq 0.025$.

(a)

$\mu = 0$, $F = 19.74$, $d_2 = 0.3084$ $\quad d_1^I = 1.2654$, $\beta = 15.79$

S	σ
0.3179	0
0.3839	0
0.4718	0
0.4938	0.0038
0.5158	0.001
0.537	0
0.625	0
0.80	0
1.1	0
1.24	0

(b)

$S = 4.9387$

μ	σ
10	-4.5×10^{-3}
1	-4.6×10^{-2}
0.1	-1.6×10^{-2}
0.03	-1.6×10^{-4}
0.025	2.4×10^{-4}
0.01	1.35×10^{-3}
10^{-4}	3.75×10^{-3}

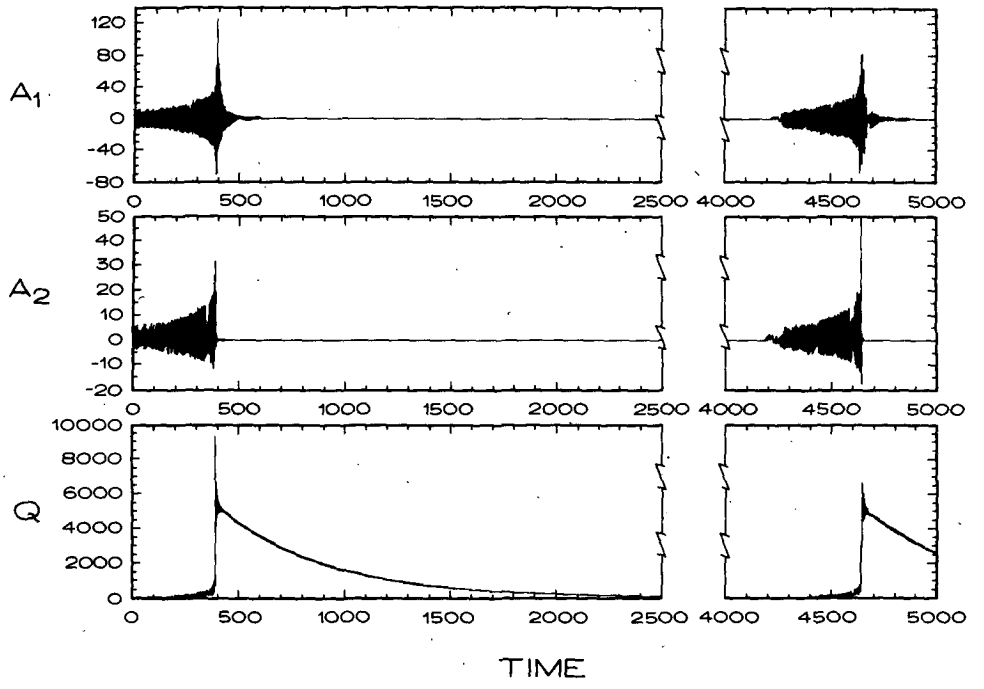

FIG. 13. For a smaller value of β, i.e., $\beta = 14.11$, where $Z_{12} < 0$ and $Z_{21} > 0$, a long relaxation oscillation occurs in which a relatively wave-free interval is separated by a burst of wave activity. The characteristic time scale for the burst is μ^{-1}, the dissipation time scale, while each burst is separated by a much larger interval (here, about 8 μ^{-1}). Here $\mu = 0.002$.

at values of μ in the range $0.025 < \mu < 0.03$ and is consistent with the occurrence of limit cycle behavior in this parameter range. It is important, however, to emphasize that persistent time-dependent solutions occur at other values of S, e.g., $0.9 < S < 1.0$, in which the steady solutions are stable.

We also found that for S outside the range (d_2, d_1^{-1}), the steady waves are linearly stable where they exist for all values of μ. Within the range of mixed wave states, the single waves are unstable for all μ.

7. Conclusions and discussions

Our principal goal in this paper was to obtain in a deductive, nontruncated fashion a model for wave–wave interaction, between unstable baroclinic waves, that is valid for small rates of dissipation where vacillation might be expected. From that point of view, the set (2.24a,b) and (2.26) are presented as a model for wave–mean flow and wave–wave interaction, which we hope transcends the particular limitations and assumptions of the β-plane model we have considered.

The model turns out to be very sensitive to two features of the analysis. First, and perhaps least expected, the nonlinear dynamics depends importantly on the *form* as well as the level of the dissipation. As we have found, dissipation, when modeled as being proportional to the perturbation of potential vorticity, acts to expunge amplitude vacillation, both periodic and chaotic, at *all* values of the dissipation parameter. Hence, the vacillations we have found in the current model are due entirely to the presence of wave–wave interaction. We also argued in section 3 that this requires a painstaking reappraisal of the f-plane layer models when interfacial friction is added, a reappraisal which is now underway and which will be reported on separately.

Obviously, the model is also sensitive to the sign and magnitude of the interaction coefficients, Z_{mn}, and the derived parameters, (d_1, d_2), which measure in a gross way the strength of the wave–wave interaction with respect to wave–mean flow interaction. In this model we have found $d_1 d_2 < 0$, implying the possibility of mixed-wave regimes and, by numerical integrations of the amplitude equations, we have verified the existence of mixed, pulsating solutions. For the cases studied in detail, chaotic behavior was found as the endpoint in parameter space when μ is decreased, whereas in the f-plane model of Pedlosky and Frenzen (1980), it was found sandwiched between steady solutions at high dissipation and periodic solutions at low dissipation.

The appearance of chaotic behavior in the wave–wave model in the limit of vanishing μ is no doubt related to the tendency of higher-order Hamiltonian systems to be nonintegrable and exhibit aperiodic behavior naturally. When $\mu = 0$ our system can be written as a fourth-order Hamiltonian system whose mixed "potential" disallows exact integration. The one-wave

inviscid problem, on the other hand, can always be integrated exactly in the inviscid limit (Pedlosky, 1970) so that the inviscid limit for the one-wave problem is periodic.

We have restricted our attention in this study almost entirely to the parameter domain in which the shear is only moderately greater than the minimum critical shear in the two-layer model, i.e., when the nondimensional β is only moderately smaller than its maximum, $F(U_1 - U_2)$. In particular, we have discussed so far only those cases where β is large enough to avoid the resonance point where the forced solutions are singular. For the values of β presented here, both Z_{12} and Z_{21} are negative, representing a mutual destabilization of each wave by its interacting sister wave.

For much smaller values of β, i.e., as the two wavenumbers k_1 and k_2 become widely separated, one of the Z_{mn} becomes positive (Fig. 2b). This asymmetry yields a somewhat bizarre history for the wave amplitudes which we, as yet, do not understand. A long-term nonlinear instability of the system occurs giving rise to the solution shown in Fig. 13. The A_1 and A_2 vacillate initially with rather high amplitude values (compare with Fig. 12) and then at $T \sim \mu^{-1}$ a steep rise in the amplitude levels of A_1 and A_2 occurs. The Q also rises precipitously (like A_n^2) and the amplitudes are quickly quenched and decay to near zero levels. Although this feature of the solution is uncertain, see below for numerical details. In fact, A_2, the amplitude of the wave for which wave–wave interaction is stabilizing ($Z_{21} > 0$), is indistinguishable from zero while A_1 slowly decays towards zero. Meanwhile, Q decays like $e^{-\mu T}$ from its high value at the amplitude burst until, about four dissipation time scales later, the mean flow is once again unstable and the process reoccurs with another burst of wave activity. When Q relaxes back to zero, the mean flow is again unstable and even A_2, never exactly zero, grows again to finite amplitude. We are frankly puzzled about the mechanism for the original burst, but its subsequent reappearance is to be expected. This relaxation oscillation of burst and decay will require further study. The time for the burst to occur seems to depend on the time step used in the calculation. We have not been able to establish numerical convergence even for a time step $\Delta t = 10^{-3}$. Therefore, we cannot be certain our numerical solution remains valid through the burst episode since the frequency of the oscillation becomes commensurate with the time step.

Acknowledgments. This research was supported in part by a grant (ATM 84-13515) from the Division of Atmospheric Sciences of the National Science Foundation. L.M.P. was also supported in part by the Natural Science and Engineering Research Council of Canada.

APPENDIX A

Parameters of the Forced Solutions

Straightforward algebra shows that the constants appearing in the forced solutions in (2.17a,b) may be written:

$$R_1 = \frac{\alpha_{12} l}{2k_{12}}\Bigg[\frac{(c_2-c_1)\partial q_1/\partial y}{(U_1-c_1)(U_1-c_2)(U_1-\omega_{12}/k_{12})} \times\left(\frac{\partial q_2/\partial y}{U_2-\omega_{12}/k_{12}}-(a_{12}{}^2+F)\right) - F\frac{\partial q_2}{\partial y}\frac{(c_2-c_1)\gamma_1\gamma_2}{(U_2-c_1)(U_2-c_2)(U_2-\omega_{12}/k_{12})}\Bigg] \times D^{-1}(k_{12}, 2l, \omega_{12}) \quad \text{(A1a,b)}$$

$$R_2 = \frac{\alpha_{12} l}{2k_{12}}\Bigg[\frac{(c_2-c_1)\partial q_2/\partial y}{(U_2-c_1)(U_2-c_2)(U_2-\omega_{12}/k_{12})} \times\left(\frac{\partial q_1/\partial y}{U_1-\omega_{12}/k_{12}}-(a_{12}{}^2+F)\right)\gamma_1\gamma_2 - F\frac{\partial q_1}{\partial y}\frac{(c_2-c_1)\gamma_1\gamma_2}{(U_1-c_1)(U_1-c_2)(U_1-\omega_{12}/k_{12})}\Bigg] \times D^{-1}(k_{12}, 2l, \omega_{12})$$

$$Q_1 = \frac{k_{12} l}{2\alpha_{12}}\Bigg[\frac{(c_2-c_1)\partial q_1/\partial y}{(U_1-c_1)(U_1-c_2)(U_1-\sigma_{12}/\alpha_{12})} \times\left(\frac{\partial q_2/\partial y}{(U_2-\sigma_{12}/\alpha_{12})}-(d_{12}{}^2+F)\right) - F\frac{\partial q_2}{\partial y}\frac{(c_2-c_1)\gamma_1\gamma_2}{(U_2-c_1)(U_2-c_2)(U_2-\sigma_{12}/\alpha_{12})}\Bigg] \times D^{-1}(\alpha_{12}, 2l, \sigma_{12}) \quad \text{(A1c)}$$

$$Q_2 = \frac{k_{12} l}{2\alpha_{12}}\Bigg[\frac{(c_2-c_1)\partial q_2/\partial y}{(U_2-c_1)(U_2-c_2)(U_2-\sigma_{12}/\alpha_{12})} \times\left(\frac{\partial q_1/\partial y}{(U_1-\sigma_{12}/\alpha_{12})}-(d_{12}{}^2+F)\right)\gamma_1\gamma_2 - F\frac{\partial q_1}{\partial y}\frac{(c_2-c_1)}{(U_1-c_1)(U_1-c_2)(U_1-\sigma_{12}/\alpha_{12})}\Bigg] \times D^{-1}(\alpha_{12}, 2l, \sigma_{12}) \quad \text{(A1d)}$$

where

$$\left.\begin{aligned}\alpha_{12} &= k_1 - k_2\\ k_{12} &= k_1 + k_2\\ \sigma_{12} &= k_1 c_1 - k_2 c_2\\ \omega_{12} &= k_1 c_1 + k_2 c_2\end{aligned}\right\} \quad \text{(A2)}$$

and

$$a_{12}^2=(k_1+k_2)^2+4l^2$$
$$d_{12}^2=(k_1-k_2)^2+4l^2. \quad \text{(A3)}$$

The function D is the critical function for the linear operator. It is defined as

$$D(k,l,\omega)\equiv\left[\frac{\partial q_1/\partial y}{U_1-\omega/k}-(a^2+F)\right]\times\left[\frac{\partial q_2/\partial y}{U_2-\omega/k}-(a^2+F)\right]-F^2 \quad \text{(A4)}$$

and vanishes only when (ω, l, k) are the frequencies and wavenumbers of a free wave. The D is generally different from zero when (k, l, ω) are the sum and difference quantities of the forced waves in (2.17a,b). The exceptional case is discussed in the text.

APPENDIX B

Constants in the Amplitude Equations

The coefficients appearing in (2.24a,b) are obtained by eliminating wavelike secular forcing terms at $O(\epsilon^3)$ in the usual manner. We give here the results of that lengthy calculation.

We first define

$$m_{12}=l\frac{\alpha_{12}+2k_2}{2}\{Q_1[-(a_2^2+F)+\gamma_2F]-[-(d_{12}^2+F)Q_1+FQ_2]\}+l\frac{k_{12}-2k_2}{2}\times\{R_1[-(a_2^2+F)+\gamma_2F]-[-(a_{12}^2+F)R_1+FR_2]\} \quad \text{(B1)}$$

$$n_{12}=-l\frac{\alpha_{12}+2k_2}{2}\{[-(d_{12}^2+F)Q_2+FQ_1]\gamma_2-[-\gamma_2(a_2^2+F)+F]Q_2\}-l\frac{k_{12}-2k_2}{2}\times\{[-(a_{12}^2+F)R_2+FR_1]\gamma_2-[-\gamma_2(a_2^2+F)+F]R_2\}$$

where the α_{mn}, k_{mn}, a_{mn}, d_{mn}, R_n, Q_n are defined in Appendix A. The numbers m_{21} and n_{21} are given by the above expression in which

$$\left.\begin{aligned}\alpha_{12}&\to-\alpha_{12}\\ k_{12}&\to k_{12}\\ \gamma_2&\to\gamma_1\\ k_2&\to k_1\end{aligned}\right\}. \quad \text{(B2)}$$

In terms of these constants

$$Z_{mn}=\frac{k_m}{F_2}\left[\frac{m_{mn}}{U_1-c_m}+\frac{\gamma_m n_{mn}}{U_2-c_m}\right]\times\left[\frac{(U_1-c_m)^2(U_1-c_m)(U_2-c_m)}{(U_1-U_2)\partial q_1/\partial y}\frac{2F^2}{a_m^4}\right]. \quad \text{(B3)}$$

while

$$Y_n=-\frac{k_n^2l^2}{a_n^4}\frac{2}{(\beta_I/F^2)}\frac{(U_1-c_n)^2(U_1-c_n)(U_2-c_n)}{(U_1-U_2)}\times\left[\left(\frac{1}{U_1-c_n}-\frac{\gamma_n^2}{U_2-c_n}\right)-\frac{1}{(2F+4l^2)}\times\left(\frac{\partial q_1/\partial y}{(U_1-c_n)^2}-\frac{\gamma_n^2\partial q_2/\partial Y}{(U_2-c_n)^2}\right)\left(1+\frac{8l^2\tanh(F/2)^{1/2}}{(4l^2+2F)(F/2)^{1/2}}\right)\right] \quad \text{(B4)}$$

and

$$X_n=\sigma_n^2/(\beta_I/F). \quad \text{(B5)}$$

The σ_n are the linear growth rates scaled by a factor of $\Delta^{1/2}$ of the two marginal waves when β is decreased by $O(\Delta)$ from the critical value for the wavenumbers (k_1, l) and (k_2, l). In that case, the σ_n are given by

$$\sigma_n^2=\frac{2k_n^2\beta F^2}{a_n^4(2F+a_n^2)^2}.$$

This makes the relative growth rates of the two waves fixed as Δ is increased. In order to allow ourselves the freedom of altering the *relative* growth rates of the two waves, we allow each of the wave numbers to be independently perturbed. Formally, to accomplish this, we need to introduce new "slow" space scales, etc. However, when it is realized that an $O(\Delta)$ shift in the wavenumber of either wave will affect only the growth rates in (2.24a,b) the result may be obtained directly from the linear dispersion relation for the inviscid problem, i.e.,

$$\frac{\sigma^2}{k^2}=\left[\frac{(U_1-U_2)^2}{4}a^4(4F^2-a^4)-\beta^2F^2\right]\Big/a^4(a^2+2F)^2. \quad \text{(B6)}$$

We now let

$$\beta=\beta_I-\Delta$$

and, for each wave

$$a^2=a_n^2+\theta_n \quad \text{(B7)}$$

from which it follows that

$$\frac{\sigma_n^2}{k_n^2}=\Delta\frac{2\beta_IF^2}{a_n^4(a_n^2+2F)^2}\left[1+2\beta_c\left(\frac{\tilde{\theta}_n}{\Delta}\right)\frac{2F^2-a_n^4}{a_n^2(4F^2-a_n^4)}\right] \quad \text{(B8)}$$

which, after removing the factor of Δ due to the scaling of T, yields the relation

$$X_n=\sigma_n^2/(\beta_I/F)$$

where

$$\sigma_n^2=\frac{2\beta_IF^2}{a_n^4(a_n^2+2F)^2}\left[1+2\beta_I\frac{\theta_n(2F^2-a_n^4)}{a_n^2(4F^2-a_n^4)}\right] \quad \text{(B9)}$$

and where $\theta_n \equiv \bar{\theta}_n/\Delta$ is an arbitrary, O(1) number. Thus, for each Δ, we can alter the relative linear growth rates at will by moving the parameter points in Fig. 4 "horizontally" in k as well as vertically in β.

REFERENCES

Hart, J. E., 1972: A laboratory study of baroclinic instability. *Geophys. Fluid Dyn.*, **3,** 181–209.

——, 1973: On the behavior of large-amplitude baroclinic waves. *J. Atmos. Sci.*, **30,** 1017–1034.

——, 1981: Wavenumber selection in nonlinear baroclinic instability. *J. Atmos. Sci.*, **38,** 400–408.

——, 1986: A model for the transition to baroclinic chaos. *Physica D*, in press.

Holopainen, E. O., 1961: On the effect of friction in baroclinic waves. *Tellus*, **13,** 363–367.

Lorenz, E. N., 1963: Deterministic non-periodic flow. *J. Atmos. Sci.*, **20,** 130–141.

Mak, M., 1985: Equilibration in nonlinear baroclinic instability. *J. Atmos. Sci.*, **15,** 2764–2782.

Mansbridge, J. V., 1984: Wavenumber transition in baroclinically unstable flows. *J. Atmos. Sci.*, **41,** 925–930.

Moroz, I. M., and P. Holmes, 1984: Double Hopf and bifurcation and quasi-periodic flow in a model for baroclinic instability on a β-plane. *J. Atmos. Sci.*, **41,** 3147–3160.

Pedlosky, J., 1970: Finite-amplitude baroclinic waves. *J. Atmos. Sci.*, **27,** 15–30.

——, 1972: Limit cycles and unstable baroclinic waves. *J. Atmos. Sci.*, **29,** 53–63.

——, 1981: The effect of β on the chaotic behavior of unstable baroclinic waves. *J. Atmos. Sci.*, **38,** 717–731.

——, and C. Frenzen, 1980: Chaotic and periodic behavior of finite-amplitude baroclinic waves. *J. Atmos. Sci.*, **37,** 1177–1196.

Romea, R. D., 1977: The effects of friction and β on finite-amplitude baroclinic waves. *J. Atmos. Sci.*, **34,** 1689–1695.